Published in final edited form as:
Signal Processing. 2008 February 1; 88(2): . doi:10.1016/j.sigpro.2007.08.011.

On approximation of smooth functions from samples of partial derivatives with application to phase unwrapping ☆

Oleg Michailovich[a,*] and **Allen Tannenbaum**[b,c]

[a]Department of Electrical and Computer Engineering, University of Waterloo, Canada N2L 3G1

[b]Schools of Electrical & Computer and Biomedical Engineering, Georgia Institute of Technology, Atlanta, GA 30332-0250, USA

[c]Department of Electrical Engineering, Technion – IIT, Israel

Abstract

This paper addresses the problem of approximating smooth bivariate functions from the samples of their partial derivatives. The approximation is carried out under the assumption that the subspace to which the functions to be recovered are supposed to belong, possesses an approximant in the form of a *principal shift-invariant* (PSI) subspace. Subsequently, the desired approximation is found as the element of the PSI subspace that fits the data the best in the $\mathbb{L}_2$-sense. In order to alleviate the ill-posedness of the process of finding such a solution, we take advantage of the discrete nature of the problem under consideration. The proposed approach allows the explicit construction of a projection operator which maps the measured derivatives into a stable and unique approximation of the corresponding function. Moreover, the paper develops the concept of *discrete* PSI subspaces, which may be of relevance for several practical settings where one is given samples of a function instead of its continuously defined values. As a final point, the application of the proposed method to the problem of phase unwrapping in homomorphic deconvolution is described.

Keywords

Derivative sampling; Approximation; Shift-invariant spaces; Phase unwrapping

1. Introduction

Medical imaging optics, acoustics, communications, and control are only a few key examples of scientific fields in which the convolution model of signal formation has long been used to account for the effect of measurement systems on signals of interest [1–5]. In all these cases, a measured signal is assumed to be a result of convolution of the original signal with the *point spread function* (PSF) of the measurement system. Since the convolution with the PSF affects the properties of the original signals, the latter needs to be recovered via an inverse procedure known as deconvolution, the most challenging version of

☆This research was supported by grants from the NSF, Air Force Office of Sponsored Research, Army Research Office, MURI, MRI-HEL, as well as by a grant from NIH (NAC P41 RR-13218) through Brigham and Women's Hospital. This work is part of the National Alliance for Medical Image Computing (NAMIC), funded by the National Institutes of Health through the NIH Roadmap for Medical Research, Grant U54 EB005149. Information on the National Centers for Biomedical Computing can be obtained from http://nihroadmap.nih.gov/bioinformatics.

*Corresponding author. Tel.: +1 519 888 4567×38247; fax: +17804921811., olegm@uwaterloo.ca, olegm@ecemail.uwaterloo.ca (O. Michailovich), tannenba@ece.gatech.edu (A. Tannenbaum).

which—termed *blind deconvolution*—refers to the case when no *a priori* knowledge about the PSF is available [6].

A variety of approaches has been proposed to cope with the task of concurrently estimating the PSF and the original signal [7]. Among these methods, an optimal balance between accuracy and computational simplicity seems to be realized by *homomorphic deconvolution* [8, Chapter 10]. The main difficultly with this approach, however, stems from the necessity to evaluate the *original* phase of the Fourier transform of the convolution mixture given a set of its measurements *wrapped* into the interval $(-\pi, \pi]$. Unfortunately, *phase unwrapping* [9] is known to be a difficult reconstruction problem, which often results in sizeable errors in the phase estimation, thereby deteriorating the overall deconvolution performance.

To avoid the unwrapping step in homomorphic deconvolution, Tribolet [10] was the first to propose the recovery of the phase of a convolution mixture by numerically integrating its first derivative. His idea has inspired a number of studies, and, in particular, the development in [11] where the original phase is recovered as the solution to a *continuous-domain* Poisson equation. It is important to note that the approach of [11] combines the process of integration with a *smoothing* procedure, thereby being capable of directly recovering the Fourier phase of the PSF (rather than that of the convolution mixture) according to the basic concept of homomorphic deconvolution.[1]

A practical limitation of the approach of [11] is the use of second-order partial derivatives as the input data. As a general rule, the higher the order of the derivative, the higher is its susceptibility to aliasing errors. Moreover, selecting a higher sampling rate by refining the lattice in the Fourier domain (so as to decrease the effect of aliasing) may result in an intolerable computational burden. Consequently, it is tempting to find a method that can recover a smoothed version of the Fourier phase of the convolution mixture from the samples of its first-order partial derivatives.

The deconvolution application considered above has been an impetus for the developments reported in this paper. In particular, the paper introduces an explicit algorithm for approximating smooth bivariate functions[2] from noisy samples of their first-order partial derivatives. Although the proposed method has been primarily aimed at solving the problem of recovering the Fourier phases, it is believed that the method presented in this paper can be used for a wider spectrum of applications. For this reason, the developments below are carried out in a general form until the experimental part of the paper, where the application of the method to the problem of (blind) homomorphic deconvolution is demonstrated.

The technique described in this paper is based on the assumption that the subspace, to which the functions of interest are supposed to belong, possesses an approximant in the form of a *principal shift-invariant* (PSI) subspace [12,13], and, hence, the desired solution can be found as an orthogonal projection onto this subspace. Unfortunately, in the continuous-domain formulation, such a projection cannot be computed in a stable way. Nevertheless, we show that a remedy can come from the fact that the problem of approximating a function from the samples of its derivatives is naturally a discrete problem. This viewpoint leads to the concept of *discrete* PSI subspaces, which admit somewhat weaker construction requirements than those used in the continuous formulation. Consequently, the discrete

[1] In homomorphic (blind) deconvolution, the PSF is recovered through estimating its log-spectrum as a smoothed version of the log-spectrum of corresponding convolution mixture. In particular, the phase of the PSF is estimated via smoothing the phase of the mixture.

[2] We restrict ourselves to the two-dimensional (2-D) case; however, this is not a serious limitation. All of the results presented below can be extended in a straightforward manner to arbitrary dimensions, but to avoid unnecessary mathematical abstraction we have not done so here.

approach makes it possible to perform the reconstruction in a stable and computationally efficient way.

The organization of the remainder of this paper is as follows. In Section 2, we briefly survey some basic properties of PSI subspaces. Many points raised in this section are well understood, and they are reviewed in order to establish the necessary notation and background for subsequent material. Section 3 introduces the notion of a discrete PSI subspace and provides a number of theoretical results serving as a basis for the proposed approximation algorithm which is specified in Section 4. A numerical implementation of the algorithm is discussed in this section as well. Finally, Section 5 gives an example of application of the method to the problem of homomorphic deconvolution, while Section 6 concludes the paper by recapping its main results.

2. Preliminaries: approximation in PSI subspaces

The concept of PSI subspaces has been extensively studied as a specific example of shift-invariant subspaces [12,13]. Given a subset $\Phi \subset \mathbb{L}_2(\mathbb{R}^d)$, the *shift-invariant* subspace generated by Φ is the smallest closed subspace of $\mathbb{L}_2(\mathbb{R}^d)$ that contains the set of all integer shifts of Φ, viz. $\text{span}\{\phi(\cdot - k) \mid \phi \in \Phi\}$, with $k \in \mathbb{Z}^d$. When Φ is a singleton, i.e., $\Phi \equiv \{\phi\}$, the resulted subspace is referred to as *principal* and the function ϕ is referred to as its *generator*. The theory of shift-invariant spaces nowadays plays an essential role in a variety of scientific fields including approximation theory [14], multiresolution approximations and wavelets [15], finite elements [16], and sampling theory [17].

2.1. Estimation of smooth functions: continuous-domain formulation

We now consider the problem of estimating a uniformly regular function $f \in \mathscr{V}$ with $\mathscr{V} \subset \mathbb{L}^2(\mathbb{R})$, given its perturbed measurements g according to

$$g = f + u. \quad (1)$$

In what follows, all functions under consideration are *real-valued* functions, with f considered as a useful signal that needs to be recovered, whereas u is regarded as noise to be rejected. Since, in most practical settings, one is usually concerned with signals of finite length, we restrict the domain of definition of f to the interval $\Omega = [0, 1]$. Moreover, the functions in (1) are also assumed to be periodic, with their basic periods supported in Ω. It should be noted that, even though the assumption of periodicity is consistent with the application we have in mind (the phases of discrete Fourier transforms (DFTs) are periodic functions), it might be a limitation in general. Fortunately, there is a way to overcome this limitation, as it is discussed later in the paper.

The problem of recovering signals from their noisy measurements has been addressed by many researches through a multitude of approaches [18]. In the current study, a *linear* approach based on a uniform smoothing is exploited. It should be noted, however, that in the case when the function to be recovered is not uniformly regular, a better solution can be provided by non-linear smoothing operators which “do not cross” boundaries between homogeneous regions of the function [19]. Nevertheless, whenever the signal to be recovered does not have singularities, uniform smoothing still remains an attractive alternative, especially from the computational point of view.

To recover a useful signal from its measurement, the signal and noise models need to be specified. For the moment, the noise u in (1) is assumed to be an arbitrary member of $\mathbb{L}_2(\Omega)$. On the other hand, the useful signal f is assumed to belong to a *periodic* PSI subspace $\mathscr{V}\Omega)$ generated by a compactly supported generator ϕ and defined as

$$\mathscr{V}(\Omega) \quad = \operatorname{span}\left\{\varphi_{J,k}^{\mathrm{per}} \overset{\mathrm{def}}{=} \sum_{l\in\mathbb{Z}} \sqrt{2^{-J}}\varphi(2^{-J}(\cdot+l)-k),\right.$$
$$\left. k=0,1,\ldots,M-1\right\}, \tag{2}$$

where $M = 2^{-J}$ with J being a *negative* integer, i.e., $J \in \mathbb{Z}^-$. It should be noted that $\mathscr{V}\Omega)$ is a finite dimensional subspace, since for any J there exist exactly M basis functions.

The subspace $\mathscr{V}\Omega)$ can be thought of as an *approximant* subspace for functions in $\mathbb{L}_2(\Omega)$, where the approximation is achieved by orthogonally projecting such functions onto $\mathscr{V}\Omega)$. In order for this projection to be stable and unique, the generator ϕ has to satisfy the *admissibility condition* which requires it to be chosen in such a way that the set $\{\phi(\cdot - k)\}_{k\in\mathbb{Z}}$ is linearly independent, and therefore constitutes a Riesz basis in the subspace it spans. This requirement is known to be fulfilled when the Fourier transform $\hat{\phi}$ of ϕ does not possess 2π-periodic zeros [13]. Moreover, if $\hat{\phi}$ has p-order zeros at each $\omega \in 2\pi\mathbb{Z}\backslash\{0\}$ (while being non-zero everywhere else), then $\mathscr{V}\Omega)$ can be used to *stably* represent polynomials of degree $(p - 1)$ on the intervals $[2^J k, 2^J(k + 1)]$, where $k = 0, 1,\ldots, M - 1$ [20]. It is worthwhile noting that from this perspective, the parameter J can be thought of as a resolution parameter in the sense that the smaller J is, the narrower is the support of $\varphi_{J,k}^{\mathrm{per}}$, and therefore the higher is the approximation order of $\mathscr{V}\Omega)$.

The properties of $\mathscr{V}\Omega)$ as an approximant are closely related to those of ϕ [12]. For the case at hand, we note that for an arbitrary $s \in \mathbb{L}_2(\Omega)$, the error of its approximation in $\mathscr{V}\Omega)$ can be shown to behave like $\|s - \mathscr{P}_{\mathscr{V}}\{s\}\| = \mathscr{O}2^{Jp}$), where $\mathscr{P}_{\mathscr{V}}$ denotes the operator of orthogonal projection onto $\mathscr{V}\Omega)$ [20]. Moreover, provided ϕ is admissible, there exists a unique *dual* generator ψ such that the sets $\{\varphi_{k,J}^{\mathrm{per}}\}_{k=0}^{M-1}$ and $\{\psi_{k,J}^{\mathrm{per}}\}_{k=0}^{M-1}$ are orthogonal, and any $s \in \mathscr{V}\Omega)$ can be represented as [17]

$$s = \sum_{k=0}^{M-1} \langle s, \psi_{k,J}^{\mathrm{per}}\rangle\, \varphi_{k,J}^{\mathrm{per}} = \sum_{k=0}^{M-1} \langle s, \varphi_{k,J}^{\mathrm{per}}\rangle\, \psi_{k,J}^{\mathrm{per}}, \tag{3}$$

where $\langle\cdot,\cdot\rangle$ stands for the standard inner product in $\mathbb{L}_2(\Omega)$. Note that the uniqueness of the construction of the dual generator ψ is guaranteed provided it obeys $\psi \in \operatorname{span}\{\phi(\cdot - k)\}$ [13,17].

The constructions in (3) are essential in defining orthogonal projections onto the target space $\mathscr{V}\Omega)$—the standard way to perform approximations [21, Chapter X]. Moreover, in many cases of practical interest, (3) provides a relatively simple and useful estimation scheme, whose properties and features have been comprehensively studied [12].

2.2. Estimation of smooth functions from noisy derivatives

The point to be addressed next is that of recovering the useful signal f from the noisy measurements q of its first-order derivative f. Denoting by $\dot{\varphi}_{J,k}^{\mathrm{per}}$ the first-order derivative $\varphi_{J,k}^{\mathrm{per}}$, the model equation is now given by

$$q = \dot{f} + u = \sum_{k=0}^{M-1} c_k \dot{\varphi}_{J,k}^{\mathrm{per}} + u, \tag{4}$$

where, as previously, u stands for the noise to be rejected.

Let $\mathcal{Q}\Omega$) denote a periodic PSI subspace spanned by $\{\dot{\varphi}^{\mathrm{per}}_{J,k}\}_{k=0}^{M-1}$. Then, the problem of estimating the useful signal *f* could be solved by first recovering the representation coefficients $\{c_k\}$ via projecting *q* onto $\mathcal{Q}\Omega$), followed by reconstructing *f* as $f=\sum_{k=0}^{M-1} c_k\varphi^{\mathrm{per}}_{J,k}$. In order to compute an orthogonal projection onto $\mathcal{Q}\Omega$), a basis dual to $\{\dot{\varphi}^{\mathrm{per}}_{J,k}\}_{k=0}^{M-1}$ should be first defined. Unfortunately, such a dual basis cannot be defined in a stable manner, inasmuch as the primal set is not a Riesz basis in the space it spans. This is because the derivative operator introduces a linear dependency between the functions of the "parent" set $\{\varphi^{\mathrm{per}}_{J,k}\}_{k=0}^{M-1}$. Specifically, the operator imposes a first-order zero on the Fourier transform of ϕ at $\omega = 0$ that makes the zeros of $\hat{\phi}$ be 2π-periodic. As a result, by the property known as "the curse of zeros" [22,23], the function ϕ cannot be an admissible generator. However, under certain conditions, the above deficiency can be alleviated within the discrete framework, as is shown in the sections that follow.

3. Discrete PSI subspaces in $\mathbb{R}^N$

3.1. Approximation of vectors in discrete PSI subspaces

From now on, it is assumed that the values of the functions under consideration are available only at the points of the set $\Omega_N=\{x_n \stackrel{\mathrm{def}}{=} n/N,\ n=0,1,\ldots,N-1\}$. (For the sake of convenience, *N* is defined to be equal to $N = 2^L$ with *L* being a *positive* integer, i.e., $L \in \mathbb{Z}^+$.) Accordingly, we reformulate the results of the preceding section for the discrete case.

Let $\mathbf{H} = \{h_{n,k}\}$ be an $N \times M$ matrix, whose columns are formed by the values of $\{\varphi^{\mathrm{per}}_{J,k}\}_{k=0}^{M-1}$ sampled at the points of Ω_N, namely $h_{n,k} \equiv \varphi^{\mathrm{per}}_{J,k}(x_n)$. Then, denoting by g_N, f_N, and u_N the *column* vectors which are comprised of the values of *g*, *f*, and *u*, respectively, evaluated at the points of Ω_N, the discrete measurement model can be defined as

$$g_N=f_N+u_N=\mathbf{H}c_M+u_N, \quad (5)$$

where $c_M \in \mathbb{R}^M$ denotes a (column) vector of the representation coefficients. We note that assuming *f* to be a member of $\mathcal{V}\Omega$) implies that f_N lies in the column space of **H**. Moreover, the projection of an arbitrary $s_N \in \mathbb{R}^N$ onto this space is stable and unique provided that the columns of **H** are linearly independent.

To find conditions which the columns of **H** have to fulfill in order to be linearly independent, we need to first introduce some more notation. Specifically, let $h_k \in \mathbb{R}^N$ be the *k*th column of **H**, with $k = 0, 1,\ldots,M - 1$. Then, denoting by $\mathcal{S}_m$: $\mathbb{R}^N \to \mathbb{R}^N$ the operator of a *left circular shift* in $\mathbb{R}^N$ by *m* discrete points, the vectors $\{h_k\}_{k=0}^{M-1}$ can be generated from the first column h_0 of **H** as $h_k = \mathcal{S}_{k\Delta}\{h_0\}$, where[3] $\Delta = N/M = 2^{J+L}$. The following proposition establishes the necessary and sufficient condition for the set $\{h_k\}_{k=0}^{M-1}$ to constitute a Riesz basis in the subspace it spans [24, Chapter 1].

Proposition 1—*Let $h \in \mathbb{R}^N$ and $\{h_k\}_{k=0}^{M-1}$ be a set of vectors generated as $h_k = \mathcal{S}_{k\Delta}\{h\}$ with $\Delta = N/M$ being a positive integer. Also let $\mathscr{F}$: $\mathbb{R}^N \to \mathbb{C}^N$ denote the operator of* DFT. *Then, the set $\{h_k\}_{k=0}^{M-1}$ is linearly independent and, hence, constitutes a Riesz basis in the subspace it spans if and only if there exist two positive constants $A>0$ and $B<\infty$ such that*

[3]Note that *L* should be greater than −*J*, otherwise Δ is not an integer and the system is undersampled.

$$A \leq \frac{1}{\Delta}\sum_{l=1}^{\Delta-1}\mathscr{S}_{lM}\{|\mathscr{F}\{h\}|^2\} \leq B, \quad (6)$$

where $|\mathscr{F}\{h\}|^2$ *is the vector obtained by point-wise absolute squaring of the values of,* $\mathscr{F}\{h\}$. *Moreover, provided* $\{h_k\}_{k=0}^{M-1}$ *is a Riesz basis, there exists a unique dual generator* $d \in \mathbb{R}^N$, *which is defined by its DFT as*[4]

$$\mathscr{F}\{d\} = \left[\frac{1}{\Delta}\sum_{l=1}^{\Delta-1}\mathscr{S}_{lM}\{|\mathscr{F}\{h\}|^2\}\right]^{-1} \cdot \mathscr{F}\{h\}, \quad (7)$$

such that $\mathscr{S}_{k1\Delta}\{h\}^{\mathrm{T}}\mathscr{S}_{k2\Delta}\{d\} = \delta_{k1,k2}$, *with* δ *being the Kronecker delta function.* (*Notice that the inverse in* (7) *is applied pointwisely*.) *Hence, the orthogonal projection* $\mathscr{P}_{\mathbf{H}}$ *of an arbitrary* $s \in \mathbb{R}^N$ onto span $\{h_k\}_{k=0}^{M-1}$ *is given by*

$$\mathscr{P}_{\mathbf{H}}\{s\} = \sum_{k=0}^{M-1}(\mathscr{S}_{k\Delta}\{d\}^{\mathrm{T}}s)\mathscr{S}_{k\Delta}\{h\}. \quad (8)$$

Proof—The proposition is proven by showing that the matrix $\mathbf{D} \in \mathbb{R}^{N \times M}$, with its *k*th column given by $\mathscr{S}_{k\Delta}\{d\}$ (where *d is* defined via (7)), constitutes a left inverse for **H**, viz. $\mathbf{D}^{\mathrm{T}}\mathbf{H} = \mathrm{I}_{M \times M}$, where $\mathrm{I}_{M \times M}$ is an $M \times M$ identity matrix. To this end, let $\tilde{\mathbf{H}}$ and $\tilde{\mathbf{D}}$ be two $N \times N$ *circulant* matrices corresponding to the vectors *h* and *d*, respectively. In addition, let $\tilde{\mathbf{W}}$ be another circulant matrix defined as $\tilde{\mathbf{W}} = \tilde{\mathbf{D}}^{\mathrm{T}}\tilde{\mathbf{H}}$. It is straightforward to verify that the first column of $\tilde{\mathbf{W}}$ is given by the *circular cross-correlation* of the vectors *d* and *h*. Moreover, being a circulant matrix, $\tilde{\mathbf{W}}$ is diagonalizable by the operator of DFT, while the eigenvalues of $\tilde{\mathbf{W}}$ are equal to the DFT of its first column *w*. The above considerations imply that

$$\begin{aligned}\mathscr{F}\{w\} &= \mathscr{F}\{d\}^* \cdot \mathscr{F}\{h\} \\ &= \left[\tfrac{1}{\Delta}\sum_{l=1}^{\Delta-1}\mathscr{S}_{lM}\{|\mathscr{F}\{h\}|^2\}\right]^{-1} \cdot |\mathscr{F}\{h\}|^2, \quad (9)\end{aligned}$$

where * stands for the complex conjugate.

Given $\tilde{\mathbf{W}}$, the matrix $\mathbf{D}^{\mathrm{T}}\mathbf{H}$ can be obtained by downsampling the columns and rows of $\tilde{\mathbf{W}}$ by the factor of Δ. Therefore, $\mathbf{D}^{\mathrm{T}}\mathbf{H}$ is a circulant matrix as well, with its first diagonal being a downsampled version of *w*. Hence, the vector of eigenvalues *v* of $\mathbf{D}^{\mathrm{T}}\mathbf{H}$ is an *aliased* version of $\mathscr{F}\{w\}$. More specifically, the vector ν is equal to the first *M* components of the vector $\tilde{\nu}$ given by

[4]Here and from now on, the dot stands for the point-wise product of vectors and matrices.

$$\begin{aligned}\tilde{\nu} &= \tfrac{1}{\Delta}\sum_{j=0}^{\Delta-1}\mathscr{S}_{jM}\{\mathscr{F}\}w\}\} \\ &= \tfrac{1}{\Delta}\sum_{j=0}^{\Delta-1}\mathscr{S}_{jM}\left\{\left[\frac{\mathbf{1}}{\boldsymbol{\Delta}}\sum_{\mathbf{l}=\mathbf{1}}^{\boldsymbol{\Delta}-\mathbf{1}}\mathscr{S}_{\mathbf{lM}}\{|\mathscr{F}\{\mathbf{h}\}|^{\mathbf{2}}\}\right]^{-\mathbf{1}}\cdot|\mathscr{F}\{\mathbf{h}\}|^{\mathbf{2}}\right\} \\ &= \left[\tfrac{1}{\Delta}\sum_{l=1}^{\Delta-1}\mathscr{S}_{lM}\{|\mathscr{F}\{h\}|^2\}\right]^{-1}\cdot\left[\tfrac{1}{\Delta}\sum_{j=0}^{\Delta-1}\mathscr{S}_{jM}\{|\mathscr{F}\{h\}|^2\}\right] \\ &= \mathbf{1}_N,\end{aligned} \quad (10)$$

where $\mathbf{1}_N \in \mathbb{R}^N$ is a column vector of ones. Therefore, $\nu = \mathbf{1}_M$ implying that $\mathbf{D}^{\mathrm{T}}\mathbf{H} = \mathbf{I}_{M\times M}$, and, hence, **D** is indeed a left inverse of **H**. Consequently, we conclude that (8) defines an orthogonal projection onto span $\{h_k\}_{k=0}^{M-1}$ (or, equivalently, onto the column space of **H**), which is well-defined and unique, provided (6) holds.

Remark—Clearly, the roles played by *h* and *d* can be interchanged. This stems directly from the fact that $\tilde{\mathbf{W}} = \tilde{\mathbf{D}}^{\mathrm{T}}\mathbf{H} = \tilde{\mathbf{H}}^{\mathrm{T}}\mathbf{D}$, and, hence, $\mathbf{H}^{\mathrm{T}}\mathbf{D} = \mathbf{D}^{\mathrm{T}}\mathbf{H} = \mathbf{I}_{M\times M}$.

Proposition 1 asserts that an estimate of the useful signal f_N in (5) may be obtained as

$$f_N \simeq \mathbf{H}\mathbf{D}^{\mathrm{T}}g_N. \quad (11)$$

How close the values of the estimate are to those of the original function depends on the amplitude of the additive noise u_N as well as on the aliasing error. Whereas the amplitude of u_N depends on the measurement conditions (and is thus not controllable), the aliasing error can be minimized by increasing *N*, and selecting ϕ with higher a zero-order *p*. In particular, for fixed *N* and *J*, the aliasing error can be reduced via choosing a compactly supported scaling function with maximal possible *p*, subject to $\mathrm{supp}\{\phi(2^{-J}x)\} \subseteq \Omega$. Thus, for example, if ϕ is chosen to be a *minimum-phase* scaling function of Daubechies [25, Chapter 6], the maximal *p* allowed in this case can be shown to be $\lfloor(2^{-J}+1)/2\rfloor$. This makes it possible to preset the parameter *p* automatically given a suitable value of *J*.

An important fact about the estimate given by (11) is that it is not invariant to cyclical shifts of the data g_N, implying that the estimate generally depends on the linear phase with which the input is received. To overcome this deficiency of (11), the cycle-spinning method of [26] may be employed. In this case, the estimation is performed for *all significant shifts*, followed by back-shifting, and subsequently, averaging all the results thus obtained. In the discrete case, the total number of such shifts is obviously equal to Δ. Moreover, it can be easily shown [27] that the translation-invariant estimate f_N^{TI} may be obtained by simply convoluting g_N with the filter *w* (whose DFT is given by (9)) normalized by Δ. Formally,

$$f_N^{\mathrm{TI}} = \frac{1}{\Delta}\sum_{l=0}^{\Delta-1}\mathscr{S}_{-l}\{\mathbf{H}\mathbf{D}^{\mathrm{T}}\mathscr{S}_l\{g_N\}\} = \Delta^{-1}(g_N * \omega). \quad (12)$$

It worthwhile noting that the filter ω is always symmetric by construction, even if the generator $\phi(x)$ is not.

Finally, we note that from the statistical point of view, (11) can be shown to be the *maximum likelihood* (ML) estimate of f_N, provided that the noise u_N is Gaussian and white [28]. If the noise covariance was equal to $\mathscr{E}\{u_N u_N^{\mathrm{T}}\} = \mathrm{U}$, the definition of the ML estimate would

require replacing the standard norm $s_1^{\mathrm{T}} s_2$ by the *weighted* norm $s_1^{\mathrm{T}} \mathrm{U}^{-1} s_2$. In such a case, the estimate f_N^{TI} given by (12) would be given by convoluting g_N with a filter depending on both ϕ and U. In this work, however, only the basic case of white Gaussian noise is addressed, since incorporating the case of correlated noises would further complicate the discussion with more technical details, while contributing little to the essence of the proposed methodology.

3.2. Estimation from sampled derivative

In what follows, we extend the results of the preceding section to the case in which a useful signal f_N has to be reconstructed from discrete noisy measurements of its first derivative. To this end, let υ_0 denote the column vector whose coordinates are equal to the values of $\dot{\phi}_{J,0}$ computed at the points of Ω_N. Further, let **K** denote an $N \times M$ matrix with columns defined by the vectors of the set $\{\mathscr{S}_{k\Delta}\{\upsilon_0\}\}_{k=0}^{M-1}$. Then, a discrete version of the continuous model (4) is given by

$$q_N = \mathbf{K} c_M + u_N, \quad (13)$$

where q_N stands for a discretized version of q, and c_M is a vector of the representation coefficients of f_N in the column space of **H**. Consequently, in the case of (13), the problem of recovering f_N amounts to the problem of estimating c_M from q_N.

From the previous discussion, it follows that a useful estimate of c_M can be obtained by projecting q_N onto the column space of **K**. Moreover, such a projection is guaranteed to be stable and unique if and only if there exits a dual generator z_0 whose DFT is given by (7) (under substitution of υ_0 instead of h), such that the $N \times M$ matrix **Z** with its columns formed by the vectors $\{\mathscr{S}_{k\Delta}\{z_0\}\}_{k=0}^{M-1}$ will constitute a left inverse for **K**. Unfortunately, such a z_0 is not guaranteed to exist. The main reason for this is "the curse of the zeros." In particular, the differentiation imposes a linear dependency on the columns of **K** which causes the coordinates of $|\mathscr{F}\{\upsilon_0\}|$ (as well as those of $\Delta^{-1}\sum_{l=0}^{\Delta-1} \mathscr{S}_{lM}\{|\mathscr{F}\{\upsilon_0\}|^2\}$) to be zero for all $n \in \Gamma \stackrel{\mathrm{def}}{=} \{kM\}_{k=0}^{\Delta-1}$. As a result, the definition of $\mathscr{F}\{z_0\}$ using (7) is not possible in the case of the derivative sampling.

A remedy to the above problem comes from the fact that for sufficiently large zero-orders p, the Fourier transform $\hat{\dot{\phi}}$ of $\dot{\phi}$ is approximately "flat" in the vicinity of $\omega = 0$. Hence, the Fourier transform of ϕ is expected to grow only linearly around $\omega = 0$. This fact implies the existence of two positive constants $A>0$, $B<\infty$ such that $A \le |\mathscr{F}\{\upsilon_0\}| \le \boldsymbol{B}$ for all $n \in \Gamma$, where $\bar{\Gamma} = \{0, 1, \ldots, N-1\} \backslash \Gamma$. This makes it possible to obtain a stable and unique approximation of the useful signal in the subspace:

$$\{s \in \mathbb{R}^N | s = \mathbf{H}c,\ \mathbf{1}_M^{\mathrm{T}} c = 0\}, \quad (14)$$

thereby suggesting that the estimation of f_N is possible *up to an additive constant*. The proposition below provides a formal description of this estimate.

Proposition 2—*Let $\upsilon \in \mathbb{R}^N$, such that $\mathbf{1}_N^{\mathrm{T}} \upsilon = 0$. Also, let* **K** *be an $N \times M$ matrix with its columns formed by the vectors $\{\mathscr{S}_{k\Delta}\{\upsilon\}\}_{k=0}^{M-1}$, where $\Delta = N/M$ is a positive integer. Finally, let Γ denote the set of indices $\{lM\}_{l=0}^{\Delta-1}$ and $\bar{\Gamma}$ be its complement in $\{0, 1, \ldots, N-1\}$. Then, if there exist two real positive constants $A>0$ and $B<\infty$, for which*[5]

$$A \leq \frac{1}{\Delta}\sum_{l=0}^{\Delta-1}\mathscr{S}_{lM}\{|\mathscr{F}\{v\}|^2\} \leq B, \quad \forall n \in \overline{\Gamma}, \quad (15)$$

then there exists a unique vector $z \in \mathbb{R}^N$, *defined by its DFT as*:

$$\mathscr{F}\{z\} = \begin{cases} \left[\frac{1}{\Delta}\sum_{l=0}^{\Delta-1}\mathscr{S}_{lM}\{|\mathscr{F}\{v\}|^2\}\right]^{-1} \cdot \mathscr{F}\{v\} & \text{for } n \in \overline{\Gamma}, \\ 0 & \text{for } n \in \overline{\Gamma}, \end{cases} \quad (16)$$

such that the orthogonal projection $\mathscr{P}_{\mathbf{K}}$ *of an arbitrary* $y \in \mathbb{R}^N$ onto $\{s \in \mathbb{R}^N | s = \mathbf{K}c, \mathbf{1}_M^{\mathrm{T}} c = 0\}$ *is given by*:

$$\mathscr{P}_{\mathbf{K}}\{s\} = \sum_{k=0}^{M-1}(\mathscr{S}_{k\Delta}\{z\}^{\mathrm{T}} y)\mathscr{S}_{k\Delta}\{v\}. \quad (17)$$

Proof—The proof of this proposition is similar to that of Proposition 1, and is accomplished by showing that the matrix $\mathbf{Z}^{\mathrm{T}}\mathbf{K}$ (where the columns of the $N \times M$ matrix $\mathbf{Z}$ are formed by the vectors of the sets $\{\mathscr{S}_{k\Delta}\{z\}\}_{k=0}^{M-1}$ constitutes an *identity operator* in $\Pi \stackrel{\mathrm{def}}{=} \{c \in \mathbb{R}^M | \mathbf{1}_M^{\mathrm{T}} c = 0\}$. We note that the latter can be defined as $\mathbf{J}_{M\times M} = \mathbf{I}_{M\times M} - M^{-1}\mathbf{1}_{M\times M}$, where $\mathbf{1}_{M\times M}$ is an $M \times M$ matrix of ones. Following exactly the same scheme that has been employed in the proof of Proposition 1, one can show that the matrix $\mathbf{Z}^{\mathrm{T}}\mathbf{K}$ is circulant (and, hence, diagonalizable by DFT), and that all but one of its eigenvalues are equal to 1, while the remaining eigenvalue (which corresponds to the constant eigenvector) is equal to zero. Therefore, multiplication of an arbitrary vector by $\mathbf{Z}^{\mathrm{T}}\mathbf{K}$ (or, equivalently, by $\mathbf{K}^{\mathrm{T}}\mathbf{Z}$) results in subtracting its mean value—the result that is obtained when multiplying the vector by $\mathbf{J}_{M\times M}$. This concludes the proof.

Proposition 2 provides the necessary tools with which a *zero-mean version* of the vector f_N can be estimated. Specifically, in the case when u_N is a white Gaussian noise and f_N belongs to the subspace defined by (14), the ML-optimal estimate $\tilde{f}_N$ of f_N can now be obtained by

$$\tilde{f}_N = \mathrm{H}\mathrm{Z}^{\mathrm{T}} q_N. \quad (18)$$

If the mean value of f_N was different from zero, then it could be represented as $f_N = \mathbf{H}c_M$, where the coefficients c_M could be decomposed as $c_M = \alpha\mathbf{1}_M + b_M$, with $b_M \in \prod$ and $\alpha \in \mathbb{R}$. In this case, given the vector $q_N = \mathbf{K}c_M$, the estimate of f_N would be given by

$$\begin{aligned} \tilde{f}_N &= \mathrm{H}\mathrm{Z}^{\mathrm{T}} q_N = \mathrm{H}\mathrm{Z}^{\mathrm{T}}\mathbf{K}c_M = \mathbf{H}\,\mathbf{J}_{M\times M}c_M \\ &= \mathbf{H}b_M = f_N - \alpha\mathbf{H}\mathbf{1}_M. \end{aligned} \quad (19)$$

If the generator ϕ obeys $\Sigma_{k\in\mathbb{Z}}\,\phi(\cdot - k) = 1$ (i.e., the shifts of ϕ form a partition of unity—the condition that is necessary for the corresponding PSI subspace to represent zero-degree polynomials), then $\mathbf{H}\mathbf{1}_M = \mathbf{1}_N$, so that $\tilde{f}_N = f_N - \alpha\mathbf{1}_N$. Moreover, since $(\mathbf{H}b_M)^{\mathrm{T}}\mathbf{1}_N = 0$, it follows that $\alpha = N^{-1}(f_N^{\mathrm{T}}\mathbf{1}_N)$. In order words, in the case $f_N^{\mathrm{T}}\mathbf{1}_N \neq 0$ the estimator (18) reconstructs the vector f_N with subtracted mean value.

[5]Here and from now on, *n* denotes the *n*th coordinate of a vector in $\mathbb{R}^N$.

Note that the above property of (18) is not a result of using a particularly poor solution method, but is inherent in the problem itself. The differentiation "filters out" the constant component of the useful signal *f*, so that its derivative contains no information about the mean value of *f*. This makes the problem of recovering *f* from its first derivative *ill-posed*, in the sense that an ambiguity arises when reconstructing the constant component of *f*. Consequently, the estimator (18) resolves this ambiguity by finding a solution that has a minimal ℓ_2-norm, which is the solution with zero mean value.

Additionally, we note that the estimate (18) is not invariant to translations of the data q_N. To overcome this difficulty, the same cycle-spinning method described in the previous section may be employed. In this case, the translation-invariant estimate $\tilde{f}_N^{\mathrm{TI}}$ of f_N can be obtained as

$$\tilde{f}_N^{\mathrm{TI}} = \frac{1}{\Delta}\sum_{l=0}^{\Delta-1} \mathscr{S}_{-l}\{\mathrm{H}\mathrm{Z}^{\mathrm{T}}\mathscr{S}_l\{q_N\}\} = \Delta^{-1}(q_N * r), \quad (20)$$

where

$$\mathscr{F}\{r\} = \begin{cases} \left[\frac{1}{\Delta}\sum_{l=0}^{\Delta-1}\mathscr{S}_{lM}\{|\mathscr{F}\{\upsilon_0\}|^2\}\right]^{-1} \\ \quad \cdot \mathscr{F}\{\upsilon_0\}\cdot\mathscr{F}^{\star}\{h_0\} & \text{for } n \in \overline{\Gamma}, \\ 0 & \text{for } n \in \Gamma, \end{cases} \quad (21)$$

with h_0 and υ_0 denoting the first columns of **H** and **K**, respectively, and ★ standing for the complex conjugation.

Finally, the definition of the reconstruction filter *r* requires one to compute the vectors h_0 and υ_0. In the case when the generator ϕ is defined analytically, this computation is straightforward. Perhaps, the most widespread example here is the family of *B*-splines [29]. Another important class of generators is the class of *refinable* functions. The functions of this class are known to obey the two-scale equation $\phi(x) = 2\Sigma_k\, a_k\phi(2x - k)$ for appropriate *interscale* coefficients $\{a_k\}$. In this case, the vectors h_0 and υ_0 may be computed as follows. Let **A** denote the convolution matrix associated with the coefficients $\{a_k\}$, and $(\Downarrow \mathbf{2})\mathbf{A}$ be the operator which removes from the matrix **A** its odd-numbered rows. Then, it can be rigorously proven that the integer values of the scaling function and its derivatives are given by the components of the eigenvectors of operator $2(\Downarrow \mathbf{2})\mathbf{A}$ associated with the eigenvalues 1 and 0.5, respectively [30, Chapter 11]. The uniqueness of the above eigenvalue problem can be guaranteed, as shown, e.g., in [31]. Subsequently, the cascade algorithm [25] can be employed to compute the values of ϕ and $\dot{\phi}$ at all $x_n = 2^{-\Delta}n$, $\forall n \in \mathbb{Z}$.

4. Reconstruction from samples of partial derivatives: 2-D case

In this section, the results derived above for the 1-D case are extended to the 2-D case. Here the useful signal is assumed to be well approximable by its projection onto the subspace $\mathscr{V}_2(\Omega \times \Omega)$ given by

$$\mathscr{V}_2(\Omega\times\Omega) = \mathrm{span}\{\Phi^J_{k_1,k_2}(x,y) \stackrel{\mathrm{def}}{=} \varphi^{\mathrm{per}}_{J,k_1}(x)\varphi^{\mathrm{per}}_{J,k_2}(y), \\ k_1,k_2 = 0,1,\ldots,M-1\}. \quad (22)$$

Note that in (22) the functions $\varphi^{\mathrm{per}}_{J,k_1}$ and $\varphi^{\mathrm{per}}_{J,k_2}$ are assumed to have the same resolution parameter $J = -\log_2 M$. This is done in order to keep the indexing as simple as possible, though in general, the resolutions along the *x*- and *y*-axes may be different.

From the discussion of the previous section, we know that recovering a function from the samples of its derivative is an ill-posed problem due to the loss of the information about the constant component of the function. In order resolve the ambiguity in recovering the constant component, the useful signal f is assumed to have zero mean value, implying that $\iint f(x, y)\,dxdy = 0$. It is worthwhile noting that the latter property of f is equivalent to requiring that the $M \times M$ matrix $\mathbf{C} = \{C_{k_1,k_1}\}$ of its representation coefficients in $\mathscr{V}_2(\Omega \times \Omega)$ obeys

$$\sum_{k_1=0}^{M-1}\sum_{k_2=0}^{M-1} C_{k_1,k_2} = \mathbf{1}_M^{\mathrm{T}}\mathbf{C}\mathbf{1}_M = 0. \quad (23)$$

In the discrete case, the sampled values of the partial derivatives q_x and q_y of f over the set $\Omega_{N\times N} = \Omega_N \times \Omega_N$ can be arranged as two $N \times N$ matrices $q^x_{N\times N}$ and $q^y_{N\times N}$, respectively, which are given by

$$\begin{aligned} q^x_{N\times N} &= \mathbf{K}\mathbf{C}\mathbf{H}^{\mathrm{T}} + u^x_{N\times N}, \\ q^y_{N\times N} &= \mathbf{H}\mathbf{C}\mathbf{K}^{\mathrm{T}} + u^y_{N\times N}, \end{aligned} \quad (24)$$

where $u^x_{N\times N}$ and $u^y_{N\times N}$ are noise terms which we assume to be mutually independent and identically distributed. Thus, the problem of estimating the samples $f_{N\times N}$ of the useful signal f amounts to the problem of estimating the representation coefficients $\mathbf{C}$. In order to proceed further, the following lemma is needed.

Lemma 1

Let $\mathbf{C} \in \mathbb{R}^{M\times M}$ *be such that* $\mathbf{1}_M^T\mathbf{C}\mathbf{1}_M = 0$. *Then*

$$\begin{aligned} \mathbf{C} &= \mathbf{J}_{M\times M}\mathbf{C} + M^{-1}\mathbf{1}_{M\times M}\mathbf{C}\mathbf{J}_{M\times M} \\ &= \mathbf{C}\mathbf{J}_{M\times M} + M^{-1}\mathbf{J}_{M\times M}\mathbf{C}\mathbf{1}_{M\times M}. \end{aligned} \quad (25)$$

Proof

The proof of the lemma is very simple, and, for this reason, only the validity of the leftmost equality will be shown below. Note that the property of $\mathbf{C}$ being a zero-mean matrix implies that $\mathbf{1}_{M\times M}\mathbf{C}\mathbf{1}_{M\times M} = 0$. Consequently, using the definition of $\mathbf{J}_{M\times M}$ one can see that

$$\begin{aligned} &\mathbf{J}_{M\times M}\mathbf{C} + M^{-1}\mathbf{1}_{M\times M}\mathbf{C}\mathbf{J}_{M\times M} \\ &\quad = \mathbf{C} - M^{-1}\mathbf{1}_{M\times M}\mathbf{C}\mathbf{J}_{M\times M} + M^{-1}\mathbf{1}_{M\times M}\mathbf{C}\mathbf{J}_{M\times M} \\ &\qquad - M^{-2}\mathbf{1}_{M\times M}\mathbf{C}\mathbf{1}_{M\times M} = C. \end{aligned} \quad (26)$$

Now, suppose for the moment that the noise terms in (24) are equal to zero. Then, multiplying $q^x_{N\times N}$ by $\mathbf{Z}^{\mathrm{T}}$ and $\mathbf{D}$ on the left and the right, respectively, would result in the matrix $\mathbf{J}_{M\times M}\mathbf{C}$. Analogously, multiplying $q^y_{N\times N}$ by $\mathbf{D}^{\mathrm{T}}$ and $\mathbf{Z}$ on the left and the right, respectively, would result in $\mathbf{C}\mathbf{J}_{M\times M}$. Consequently, using the results of Lemma 1, in the noise-free case, the coefficients of (zero-mean) $\mathbf{C}$ can be uniquely recovered using *either* of the following two relations:

$$\mathbf{C} = \boldsymbol{Z}^{\mathrm{T}}q^x_{N\times N}\mathbf{D} + M^{-1}\mathbf{1}_{M\times M}\mathbf{D}^{\mathrm{T}}q^y_{N\times N}\boldsymbol{Z} \quad (27)$$

or

$$\mathbf{C}=\mathbf{D}^{\mathrm{T}}q^{y}_{N\times N}\boldsymbol{Z}+M^{-1}\boldsymbol{Z}^{\mathrm{T}}q^{x}_{N\times N}\mathbf{D}\mathbf{1}_{M\times M}. \quad (28)$$

When the noises $u^{x}_{N\times N}$ and $u^{y}_{N\times N}$ are different from zero, the estimates of **C** given by (27) and (28) are not in general equal. In this case, an *average* estimate of **C** which is obtained as the arithmetic mean of (27) and (28) seems to be a reasonable solution, under the conditions that the noises $u^{x}_{N\times N}$ and $u^{y}_{N\times N}$ have comparable variances. The average estimate $\overline{\mathbf{C}}$ can be shown to be given by

$$\overline{\mathbf{C}}=\frac{1}{2}(\boldsymbol{Z}^{\mathrm{T}}q^{x}_{N\times N}\mathbf{D}\tilde{\mathbf{J}}_{M\times M}+\tilde{\mathbf{J}}_{M\times M}\mathbf{D}^{\mathrm{T}}q^{y}_{N\times N}\boldsymbol{Z}), \quad (29)$$

where $\tilde{\mathbf{J}}_{M\times M}=\mathbf{I}_{M\times M}+M^{-1}\mathbf{1}_{M\times M}$. As a result, the discrete values of the useful signal at the points of $\Omega_{N\times N}$ can be estimated as

$$\begin{aligned}\tilde{f}_{N\times N} &=\mathbf{H}\overline{\mathbf{C}}\mathbf{H}^{\mathrm{T}}\\ &=\tfrac{1}{2}\mathbf{H}(\boldsymbol{Z}^{\mathrm{T}}q^{x}_{N\times N}\mathbf{D}\tilde{\mathbf{J}}_{M\times M}+\tilde{\mathbf{J}}_{M\times M}\mathbf{D}^{\mathrm{T}}q^{y}_{N\times N}\boldsymbol{Z})\mathbf{H}^{\mathrm{T}}.\end{aligned} \quad (30)$$

Note that the estimate (30) can be proven to be optimal in the ML sense provided that the noises $u^{x}_{N\times N}$ and $u^{y}_{N\times N}$ are independent and identically distributed white Gaussian noise processes.

Once again, we note that the estimate (30) has the drawback of being non-invariant to translations (shifts) of data. In the 2-D case, the total number of such shifts *concurrently* applied to $q^{x}_{N\times N}$ and $q^{y}_{N\times N}$ is equal to Δ^2. In order to render the estimate of $f_{N\times N}$ translation invariant, the cycle-spinning method from the previous section can be used once again. As in the 1-D case, the translation-invariant estimation can be computed via linear filtering. The derivation of this result is somewhat tedious, and for this reason it is omitted here. Hence, only the final formulas, needed for practical implementation of the proposed method, are provided below.

Let $p^{x}_{N\times N}$ be an $N\times N$ matrix with identical rows equal to $r*(q^{x}_{N\times N}\mathbf{1}_{N})/N$, where r is defined by (21). In the same manner, let $p^{y}_{N\times N}$ be an $N\times N$ matrix having identical columns equal to $r*(1^{\mathrm{T}}_{N}q^{y}_{N\times N})/N$. Then, the translation-invariant estimate $\tilde{f}^{\mathrm{TI}}_{N\times N}$ of $f_{N\times N}$ can be shown to be given by

$$_{x}+q^{y}_{N\times N}*\chi_{y}+p^{x}_{N\times N}+p^{y}_{N\times N}), \quad (31)$$

where the filters χ_x and χ_y are defined via their 2-D DFT (denoted below by $\mathscr{F}_{\text{2-D}}$) as follows:

$$_{x}\}=\mathscr{F}\{r\}\mathscr{F}\{w\}^{\mathrm{T}},\ \mathscr{F}_{2-\mathrm{D}}\{\chi_{y}\}=\mathscr{F}\{w\}\mathscr{F}\{r\}^{\mathrm{T}}. \quad (32)$$

The above expressions imply that the overall complexity of computing the translation-invariant estimate of $f_{N\times N}$ from the samples of its partial derivatives is logarithmic, i.e., $\mathcal{O}$ $N^2\log_2 N$).

The filters χ_x and χ_y are supposed to be pre-computed and stored before the estimate of $f_{N\times N}$ is initialized. Note that the properties of these filters are defined by those of the generator ϕ as well as by the parameter J. In most of the experimental results of the following section, the *cubic* B_3-spline was used as a generator (suggesting $p = 4$).

5. Results: phase unwrapping for homomorphic deconvolution

As it was mentioned in Introduction, the proposed method for estimating bivariate functions from the samples of their partial derivatives originated from a practical problem of recovering the Fourier phases of PSFs as part of homomorphic deconvolution. Accordingly, the experimental results reported in this section are related to this application.

5.1. Reference methods for phase unwrapping

Let $\Phi_{N\times N}$ be a matrix of discrete values of the phase of a complex function evaluated over $\Omega_{N\times N}$. In addition, let $\Psi_{N\times N}$ be a *wrapped* version of $\Phi_{N\times N}$ defined as $\Psi_{N\times N} = \mathscr{W}\{\Phi_{N\times N}\}$ with $\mathscr{W}$ being the wrapping operator. Then, denoting by $\mathscr{D}_x$ and $\mathscr{D}_y$ the operators of the "column" and "row" partial differencing, respectively, it can be shown that if

$$\max\{|\mathscr{D}_x\{\Phi_{N\times N}\}|, |\mathscr{D}_y\{\Phi_{N\times N}\}|\} < \pi, \quad (33)$$

then the partial differences of $\Phi_{N\times N}$ can be recovered from those of $\Psi_{N\times N}$ as [9]

$$\begin{aligned} \mathscr{D}_x\{\Phi_{N\times N}\} &= \mathscr{W}\{\mathscr{D}_x\{\Psi_{N\times N}\}\}, \\ \mathscr{D}_y\{\Phi_{N\times N}\} &= \mathscr{W}\{\mathscr{D}_y\{\Psi_{N\times N}\}\}. \end{aligned} \quad (34)$$

Consequently, the estimated partial differences $\mathscr{D}_x\{\Phi_{N\times N}\}$ and $\mathscr{D}y\{\Phi_{N\times N}\}$ can be used to compute the Laplacian of $\Phi_{N\times N}$, followed by estimating the latter as the solution to a *discrete-domain* Laplace equation subject to periodic boundary conditions. Note that this solution is unique provided $\Phi_{N\times N}$ has zero-mean, and, moreover, the solution can be shown to globally minimize the ℓ_2-norm between its partial differences and the partial differences estimated according to (34) [32]. For the latter reason, the above approach to phase unwrapping is commonly referred to as the *least squares* (LS) method.

Note that in the case of Fourier phases, the LS method is capable of recovering the values of $\Phi_{N\times N}$ *precisely* provided the condition (33) is met. Consequently, if $\Phi_{N\times N}$ was the Fourier phase of a convolution mixture, then its LS-estimate could be further used to estimate the phase of the associated PSF by properly smoothing the former (as it is envisaged within the framework of homomorphic deconvolution). The smoothing, in turn, could be achieved through projecting the LS-estimate of $\Phi_{N\times N}$ onto the subspace (22), which would have amounted to multiplying the DFT of the estimate by $\mathscr{F}\{w\}$, $\mathscr{F}\{w\}^{\mathrm{T}}$ (with w defined via (9)), had one required the result to be translation invariant. (In the sequel, we refer to such a solution as a *smoothed least squares* (SLS) solution.)

Unfortunately, the performance of both LS and SLS methods deteriorates dramatically, when the condition (33) breaks down. Some standard ways to circumvent this difficulty include either "masking out" or "going round" the points, at which the condition (33) appears to be violated, when the Laplace equation is being integrated [9]. Neither of these solutions, however, is known to be reliable and computationally efficient at the same time. On the other hand, as long as Fourier phases are considered, a much simpler alternative would be to recover $\Phi_{N\times N}$ from the samples of its partial derivatives, as it is described in this paper. We note that the partial derivatives of the phase Φ of a 2-D Fourier transform $\hat{f}$ can be computed in their *unwrapped* form according to

$$\frac{\partial \Phi(\omega_1,\omega_2)}{\partial \omega_k} = \Im\left\{ \frac{\mathbf{1}}{\widehat{\mathbf{f}}(\omega_1,\omega_2)} \frac{\partial \widehat{\mathbf{f}}(\omega_1,\omega_2)}{\partial \omega_{\mathbf{k}}} \right\},\ k \in 1,2, \quad (35)$$

where $\Im$ stands for the imaginary part.[6] Since the proposed method is designed to integrate the partial derivatives *directly* over a subspace of smooth functions (which seems to be an additional advantage in the context of homomorphic deconvolution), it is referred below to as the *smoothing integration* (SI) method.

In order to assess the experimental results in a quantitative manner, the normalized *mean squared error* (NMSE) was employed as a comparative measure in this paper. Denoting by $s_{N\times N}$ the original 2-D discrete signal to be recovered, and by $\tilde{S}_{N\times N}$ its estimate, the NMSE can be defined as

$$\mathrm{NMSE} = \mathscr{E}\left\{ \frac{||\mathbf{s}_{\mathbf{N}\times\mathbf{N}} - \tilde{\mathbf{s}}_{\mathbf{N}\times\mathbf{N}}||_{\mathrm{F}}}{||\mathbf{s}_{\mathbf{N}\times\mathbf{N}}||_{\mathrm{F}}} \right\}, \quad (36)$$

with $\|\cdot\|_{\mathrm{F}}$ standing for the Frobenius norm. Note that, in the current paper, each expectation $\mathscr{E}$ was approximated by corresponding sample mean based on the results of 200 independent trials.

5.2. Estimation of simulated Fourier phases

In the experimental part of this paper, the performances of the LS, SLS, and SI methods are first compared using the Fourier phases of computer-generated *random* sequences. We note that, given an $N_1 \times N_2$ sequence $S_{N_1\times N_2}$, its Fourier phase can be defined as a restriction of the corresponding *z*-transform to the unit sphere. As is well-known, it is generally impossible to compute the original (i.e., unwrapped) Fourier phase of $S_{N_1\times N_2}$ by means of closed-form expressions. On the other hand, a univariate polynomial can always be represented as a product of first-order factors, thus allowing its phase to be computed as the sum of all the elementary phases "contributed" by the monomials. Moreover, as the phases of the monomials admit a closed-form analytical expression, it is rarely a problem to compute the Fourier phases of 1-D sequences in their original form [33]. For the above reasons, the random sequences used in this part of the experimental study were generated in a *separable* way, viz. in the form of $s_{N_1\times N_2} = s_{N_1} s_{N_2}^{\mathrm{T}}$ (where S_{N_1} and S_{N_2} are two random column vectors of dimensions N_1 and N_2, respectively). Note that, in this case, the Fourier phase of a 2-D sequence is completely defined by the phases of its 1-D "column" and "row" components.

The size of the simulated sequences was taken to be 32 × 32. Moreover, since most of the PSFs behave as band-pass filters, the zeros of their *z*-transforms should be distant from the unit circle/sphere, as least within their pass-band. To mimic such a behavior, the zeros of the *z*-transforms of the simulated sequences were not allowed to fall within the annulus $0.98 \le |z| \le 1{:}02$. Fig. 1 shows the distribution of the zeros of the *z*-transforms corresponding to the "column" and "row" components of a typical simulated sequence.

Table 1 summarizes the results of phase estimation obtained by using the LS, SLS, and SI methods for different values of SNR.[7] In this experiment, the generator ϕ was defined to be a cubic B_3-spline, the resolution J was set to be equal to −5, and all the Fourier transforms

[6]The partial derivatives of $\hat{f}$ can be efficiently computed by applying the DFT to linearly weighted versions of its spatial-domain counterpart [8].

[7]Note that, throughout the simulation study, the additive noise was taken to be white and Gaussian.

were evaluated over an $N \times N$ rectangular lattice with $N = 256$. One can see that the LS method is capable of virtually perfectly recovering the original phase from its wrapped values for relatively high values of SNR. However, when the increasing amplitudes of the noise make the condition (33) fail, the performance of the LS method deteriorates considerably, with its NMSE exceeding 32% at SNR = 10 dB. Analogously, the SLS method results in relatively low values of NMSE (about 1%) for relatively high values of SNR. It is worthwhile noting that the error here is mainly due to the *approximation* associated with projecting the solution onto the predefined PSI subspace. Unfortunately, this method is also susceptible to violation of the condition (33), with its error approaching 26% when SNR goes down to 10 dB. On the other hand, the NMSE values of the proposed SI method increase only moderately with decreasing of SNR, thereby exhibiting a dependency on the noise level alone. Specifically, at 10 dB noise level, the error of the SI method is about 1.6%.

Fig. 2 illustrates the above results by demonstrating the original phase of a simulated random sequence, its noise-contaminated version (SNR = 40 dB), as well as the resulting SLS and SI estimates in Subplots A1–A4, respectively. One can see that, for this level of noise, both methods result in the estimates which are virtually indistinguishable from the original phase. However, the results obtained for SNR = 10 dB (which are shown in Subplots B1–B4 of Fig. 2) clearly demonstrate the drawbacks of the SLS approach that provides a much noisier reconstruction as compared to the SI method.

Since there is little conceptual difference between the LS and SLS methods, and since the latter is more relevant to the technique of smooth estimation which we will need for the application we have in mind, only the SLS and SI methods will be compared from now on. Specifically, the next question to be addressed is that of the influence of the parameter J on the quality of phase reconstruction. It should be noted that, since J controls the "bandwidth" of the estimation, the NMSE values are expected to increase whenever the corresponding PSI subspace is either too "narrow-banded" or too "broad-banded" for representing a specific phase at hand.

Table 2 shows the results obtained by using the SLS and SI methods for different values of J. In this experiment, the generator ϕ was defined to be a cubic B_3-spline, whereas N and SNR were set to be equal to 256 and 15 dB, respectively. One can observe that both methods minimize the NMSE at $J = -5$. At the same time, the error goes up for smaller values of J, as the increased bandwidth allows too much noise into the solution. In a similar manner, the error increases for higher values of J as a result of overly smoothing the solution. Thus, one can conclude that the PSI subspace corresponding to $J = -5$ optimally represent the phases used in this simulation study. We note that the above value of J can by no means be regarded as *universally* optimal, as it strongly depends on the smoothness properties of the function that needs to be recovered. Consequently, finding an optimal value of J turns out to be an issue by itself. We discuss some possible solutions to this problem in the concluding section of this paper.

From the above discussion, it stems that the main drawback of both the LS and SLS methods is related to their property of being dependent on the condition (33) which requires the absolute values of the partial differences of the original phase Φ to be smaller than π. Since the differences can be made arbitrary small by refining the (sampling) lattice in the Fourier domain, one can expect that for a sufficiently large value of N, the performances of the SLS and SI methods should be similar. This expectation is supported by the results tabulated in Table 3 that compares the performances of the SLS and SI methods for different values of N. In this experiment, the generator was also defined as a cubic B_3-spline, J was set to be equal to −5, while SNR was taken to be 15 dB. One can see that, for $N = 64$, the SLS method

performs considerably worse (NMSE is about 13%) as compared to the SI method (NMSE is about 2.4%). Note that in the former case, the error is mainly caused by inaccuracies in computing the partial differences of the phases (as a result of violation of the condition (33)), while in the latter case, the error is predominantly due to aliasing. For $N = 256$, the SI method still results in the NMSE value that is about three times smaller than the error produced by the SLS approach. However, for $N = 512$, both methods achieve virtually identical error rates. Since the computational complexity of all the methods under consideration is logarithmic, one can conclude that the proposed SI approach may be advantageous in situations when the computational time is of particular importance.

We conclude this part of the experimental study with investigating the dependency of the performance of the SI method on the approximation power of the PSI subspace as controlled by the parameter p. To this end, the values of N, J, and SNR were set to be equal to 256, −5, and 15 dB, respectively, while the generator ϕ was defined in the form of B-splines of orders 2, 3, 4, and 5 (corresponding to $p = 3,\ldots,6$, respectively) [34]. The resulting values of the NMSE are shown in Table 4. One can see that, as predicted by the theory, the PSI subspaces constructed using more regular splines are capable of better representing the simulated phases. The dependency on p, however, seems to be relatively mild.

5.3. Phase reconstruction in ultrasound imaging

In this part of the experimental study, we restrict the discussion to a specific class of PSFs which characterize the image formation in ultrasound imaging. In particular, we investigate the influence of the phase estimation error on the shape of such PSFs in the spatial domain. In order to generate these PSFs, the Field-II® software package was used [35].

A set of the PSFs corresponding to a typical configuration of a (phased-array) ultrasound transducer were collected in the form of 64 × 64 matrices. Subsequently, the obtained PSFs were contaminated by white Gaussian noise giving rise to the SNR of 15 dB. Finally, the PSFs were recovered using the *true* magnitudes of their Fourier transforms, while the phases of the estimated PSFs were reconstructed by means of the SLS and SI methods. The reconstruction was performed with $\phi = B_3$ and $J = 5$, while N was varied between 64 and 512 samples. The NMSE values of the resulting PSF estimates are summarized in Table 5. One can see that for $N = 64$ (i.e., in the case when no over-sampling is used), the errors of the PSF estimation using the SLS approach is almost five times higher than the error related to the SI method, which is equal to 4.76%. When the Fourier transforms are oversampled by the factor of 4 ($N = 256$), the error of the SI-based reconstruction is still about two times smaller than the error of the SLS-based reconstruction. It is only for $N = 512$ that both methods result in almost identical error of about 1.3%. Apparently, in this case, the sampling density in the Fourier domain becomes high enough for the condition (33) to hold. Hence, one can conclude that the proposed SI method can be employed for recovering the PSF with a relatively high accuracy for considerably lower values of N (as compared to the SLS approach), which makes it more useful for applications in which the speed of computations is a key issue. Fig. 3 exemplifies the above results by showing the original PSF (leftmost subplot) and its estimates obtained using the SLS and SI methods (central and rightmost subplots, respectively) for $N = 128$. (Note that the PSFs here are shown as gray-scale images, with the black and white colors corresponding to their smallest negative and the largest positive values, respectively.) In this case, a visual comparison easily reveals the fact that, due to the errors in phase estimation, the SLS-based reconstruction fails to recover the correct support of the PSF.

Finally, the phase estimation methods under consideration were compared using real-life data. To this end, a set of ultrasound images were acquired from a tissue-mimicking phantom using a single-element, 3.5MHz transducer (Panametrics V383, Waltham, MA) for

both transmission and reception. The data acquisition was performed by steering the transducer in the lateral direction with resolution of 0.5 mm. The acquired data were sampled at 25MHz (using CompuScope 14100, GAGE Applied, Inc.) with 14 bits resolution. An example of the demodulated envelope of a segment of an acquired image is shown in the leftmost subplot of Fig. 4. In addition, measurements of the corresponding PSF were performed by imaging a point target (a steel wire) in a water tank using the same experimental setup. The measured PSF is shown in the upper subplot of the leftmost column of subplots in Fig. 4.

Subsequently, the multitude of the Fourier transform of the PSF was estimated using the method detailed in [36], while the phase of the PSF was recovered using both the SLS and SI methods. The oversampling factor was set to be equal to 2 (implying twice as many samples in the Fourier domain as it was in the spatial domain). The optimal value of −4 for the resolution parameter J was found empirically as a minimizer of the resulting estimation error. The generator ϕ was defined again to be a cubic B_3-spline.

Two examples of the PSF estimation are depicted in the two lower (leftmost) subplots of Fig. 4. One can see that while SI-based method succeeds well in recovering the PSF shape and support information, the SLS-based method suffers from “phase” errors, which appear as “warping” and “smearing” of the estimated PSF shape. For this case, the NMSE values for the SLS and SI methods were found to be equal to 14.2% and 5.8%, respectively.

6. Discussion and conclusions

A method for estimating the values of smooth functions from the (noisy) samples of their partial derivatives has been presented. The proposed estimation scheme is based on the assumption that the function which needs to be recovered is approximable in a properly defined PSI subspace. In this case, a reasonable solution to the estimation problem can be found as the element of the PSI subspace that “fits” the data the best in the $\mathbb{L}_2$-sense. Unfortunately, finding such a solution in the case of continuous-domain formulation is an ill-posed problem, which is a direct consequence of the fact that the derivative operator is generally not injective.

The above difficulty has been overcome by noting that as long as sampled signals are considered, the corresponding reconstruction problem is discrete in nature. Consequently, via appropriately adjusting the notion of PSI subspaces to the discrete setting, it becomes possible to define a way to achieve a stable and unique reconstruction by means of only a few filtering operations. Thus, besides introducing a computationally efficient method for smooth integration, we believe that this study provides some useful insight into the problem of the construction of discrete integrators with controllable smoothness properties.

The estimation error provided by the proposed method depends on the severity of both the noise and aliasing. While the size of the noise depends on measurement conditions, the effect of aliasing can be reduced via increasing the sampling rate as controlled by N. It should be noted, however, that an unbounded increase of N can lead to instability, since the discrete formulation converges to the continuous case as $N \to \infty$. From the point of view of the theory of Riesz bases, the instability is caused by the lower bound A in (15) approaching zero. Therefore, it is interesting to find the rate at which the above convergence occurs. In this connection, we note that the Fourier transform of $\dot{\varphi}^{\mathrm{per}}_{J,0}$ is equal to $\sqrt{2^{-J}}_l(2^J\omega)\widehat{\varphi}(2^J\omega)$, with $\widehat{\phi}$ denoting the Fourier transform of ϕ, as before. Since, for most of the generators ϕ with sufficiently high orders p, their Fourier transforms are approximately constant in vicinity of $\omega = 0$, one has $\sqrt{2^{-J}}_l(2^J\omega)\widehat{\varphi}(2^J\omega) \approx \sqrt{2^{-J}}_l(2^J\omega)\widehat{\varphi}(0)$ in a small neighborhood

of the origin, which implies that the Fourier transform of $\dot{\varphi}^{\mathrm{per}}_{J,0}$ changes *linearly* around ω = 0. Therefore, for sufficiently high values of *N*, the lower bound *A* should be expected to be of the order of $\mathcal{O}N^{-1}$). Fortunately, in practical settings, the values of *N* are always finite, which guarantees the stability of the reconstruction.

The proposed estimation method has been developed under the assumption that the functions to be recovered are periodic. This assumption, however, might be a limitation in the cases when the periodicity cannot be taken advantage of. To overcome this deficiency, we first note that the proposed integration method is completely defined by the filters *w* and *r*, as specified by (9) and (21), respectively. Given the DFTs of these filters, it is rarely a problem to find either FIR or IIR filters of finite lengths, the transfer functions of which will approximate $\mathcal{F}\{w\}$ and $\mathcal{F}\{r\}$ to a reasonably high precision [37]. Subsequently, such filters could be used instead of *w* and *r* to perform the reconstruction subject to necessary boundary conditions, as required by an application at hand. It should also be noted that the filters *w* and *r* are low-pass filters by construction, and therefore they are capable of suppressing the influence of out-of-band noises on the solution. Moreover, the absolute values of the frequency responses of the filters can be shown to be bounded by 1, thereby suggesting that the filters will never amplify the noise within their pass-bands. However, while the frequency response of *w* is virtually “flat” within its pass-band, the frequency response of the *integrating filter r* tends to amplify lower frequencies more than higher. Consequently, the corresponding “coloring” of the within-band noise should be expected.

In the experimental part of this paper, the application of the proposed method to the problem of phase unwrapping in homomorphic deconvolution was described. Since the method is designed to integrate the partial derivatives of the phase over a subspace of smooth, relatively slow-varying functions, it can be used to recover the phase of a PSF directly from that of the corresponding convolution mixture. We have seen, however, that the phase estimation error is generally dependent on the resolution parameter *J*. To predefine an optimal value of *J*, one could first *predict* the shape of the PSF based on either preliminary measurements or an analytical model. Given the predicted PSF, its separable approximation could then be computed by means of the singular value decomposition, followed by computing the Fourier phase of the approximation in the very same way as we used to compute the test phases in Section 5.2. Finally, the optimal *J* could be found as a minimizer of the distance between the approximated phase and its projection onto the corresponding PSI subspace. Alternatively, an optimal value of *J* could be found by performing blind deconvolution for a range of different values of *J*, followed by choosing the one that provides the best deconvolution result. In practice, however, we observed that both above-mentioned approaches resulted in the same optimal values of *J*, and, for this reason, we preferred the first one for its being more direct and less time consuming.

Apart from testing the performance of the proposed method under different conditions, the method has also been compared with the standard LS solution, which was recently applied to the problem of homomorphic deconvolution in ultrasound imaging in [38]. It was demonstrated that the proposed method is capable of recovering the Fourier phase of the PSF of ultrasound scanners with a considerably higher accuracy as compared to [38]. This suggests that the proposed method may be useful for some important practical applications in medical imagery.

References

1. Taxt T. Restoration of medical ultrasound images using two-dimensional homomorphic deconvolution. IEEE Trans. Ultrason. Ferroelect. Freq. Contr. 1995 Jul; 42(4):543–554.

2. Blass, WE. Deconvolution of Absorption Spectra: Deconvolution of Infrared and Other Types of Spectra. New York: Academic Press; 1982.
3. Gaspin J, Goertner J, Blatstein I. The determination of acoustic source levels for shallow underwater explosions. J. Acoust. Soc. Amer. 1979 Nov; 66(5):1453–1462.
4. Haykin, S. Unsupervised Adaptive Filtering. New York: Wiley-Inter-science; 2000.
5. Mendel, J. Optimal Seismic Deconvolution: An Estimation Based Approach. New York: Academic Press; 1983.
6. Dimri, V. Deconvolution and Inverse Theory. Elsevier Health Sciences; 1992.
7. Vogel, C. Computational Methods for Inverse Problems. Philadelphia, PA: SIAM; 2002.
8. Oppenheim, AV.; Schafer, RW. Discrete Time Signal Processing. London: Prentice-Hall; 1989.
9. Ghiglia, DC.; Pritt, MD. Two-dimensional Phase Unwrapping: Theory, Algorithms, and Software. New York: Wiley-Interscience; 1998.
10. Tribolet JM. A new phase unwrapping algorithm. IEEE Trans. Acoust. Speech Signal Process. 1977 Apr.(2):170–177. ASSP-25.
11. Michailovich O, Adam D. Phase unwrapping for 2-D blind deconvolution of ultrasound images. IEEE Trans. Med. Imaging. 2004 Jan; 23(1):7–25. [PubMed: 14719683]
12. de Boor C, Ron A. Fourier analysis of the approximation power of principal shift-invariant spaces. Constr. Approx. 1992; 8:427–462.
13. Ron, A. Introduction to shift-invariant spaces: linear independence, in: Multivariate Approximation and Applications. Cambridge: 2001. p. 112-151.
14. Dyn, N.; Leviatan, D.; Levin, D.; Pinkus, A., editors. Multivariate Approximation and Applications. Cambridge: Cambridge University Press; 2001.
15. Carnicer J, Dahmen W, Pena JM. Local decomposition of refinable spaces and wavelets. Appl. Comp. Harm. Anal. 1996 Apr; 3(2):127–153.
16. de Boor C. Multivariate piecewise polynomials. Acta Numer. 1993 Feb.1:65–109.
17. Aldroubi A, Grochenig K. Non-uniform sampling and reconstruction in shift-invariant spaces. SIAM Rev. 2001; 43(4):585–620.
18. Ahmed, NU. Linear and Nonlinear Filtering for Engineers and Scientists. Singapore: World Scientific; 1999.
19. Donoho D. De-noising by soft-thresholding. IEEE Trans. Inform. Theory. 1995 May; 41(3):613–627.
20. Strang, G.; Fix, G. A Fourier analysis of the finite element variational method. In: Geymonat, G., editor. Constructive Aspects of Functional Analysis. 1973. p. 793-840.
21. Mallat, S. A Wavelet Tour of Signal Processing. New York: Academic Press; 1998.
22. de Boor C, DeVore R, Ron A. Approximation from shift-invariant subspaces in $\mathbb{L}_2(\mathbb{R}^d)$. Trans. Amer. Math. Soc. 1994; 341:787–806.
23. Ron A, Chen Z. Frames and stable bases for shift-invariant subspaces of $\mathbb{L}_2(\mathbb{R}^d)$. Canad. J. Math. 1995; 47:1051–1094.
24. Christensen, O. An Introduction to Frames and Riesz Bases. Basel: Birkhauser; 2003.
25. Daubechies, I. Ten Lectures on Wavelets. Philadelphia, PA: SIAM; 1992.
26. Donoho, D.; Coifman, R. Translation-invariant de-noising, Technical Report 475. Department of Statistics, Stanford University; 1995 May.
27. Michailovich O, Adam D. Shift-invariant, DWT-based projection method for estimation of ultrasound pulse power spectrum. IEEE Trans. Ultrason. Ferroelect. Freq. Contr. 2002 Aug; 49(8): 1060–1072.
28. Barkat, M. Signals: Detection and Estimation. Boston: Artech House; 1991.
29. Schoenberg IJ. Contribution to the problem of approximation of equidistant data by analytic functions. Quart. Appl. Math. 1946 Feb.4:45–99.
30. Strang, G.; Nguyen, T. Wavelets and Filter Banks. Wellesley, MA: Wellesley-Cambridge Press; 1996.
31. Dahmen W, Micchelli CA. Using the refinement equation for evaluating integrals of wavelets. SIAM J. Numer. Anal. 1993 Apr; 30(2):507–537.

32. Rektorys, K. Variational Methods in Mathematics, Science, and Engineering. Dordrecht: Reidel; 1980.

33. Steiglitz K, Dickinson B. Phase unwrapping by factorization. IEEE Trans. Acoust. Speech Signal Process. 1982 Dec; 30(6):984–991.

34. Unser M. Sampling—50 years after Shannon. Proc. IEEE. 2000 Apr; 88(4):569–587.

35. Jensen JA. FIELD: a program for simulating ultrasound systems. Med. Biol. Eng. Comput. 1996; 34(1):351–353. [PubMed: 8945858]

36. Michailovich O, Adam D. A novel approach to 2-D blind deconvolution in medical ultrasound. IEEE Trans. Med. Imaging. 2005 Jan.24(1)

37. de Freitas, JM. Digital Filter Design Solutions. Boston: Artech House; 2005.

38. Taxt T, Frolova G. Noise robust one-dimensional blind deconvolution of medical ultrasound images. IEEE Trans. Ultrason. Ferroelect. Freq. Contr. 1999 Mar; 46(2):291–299.

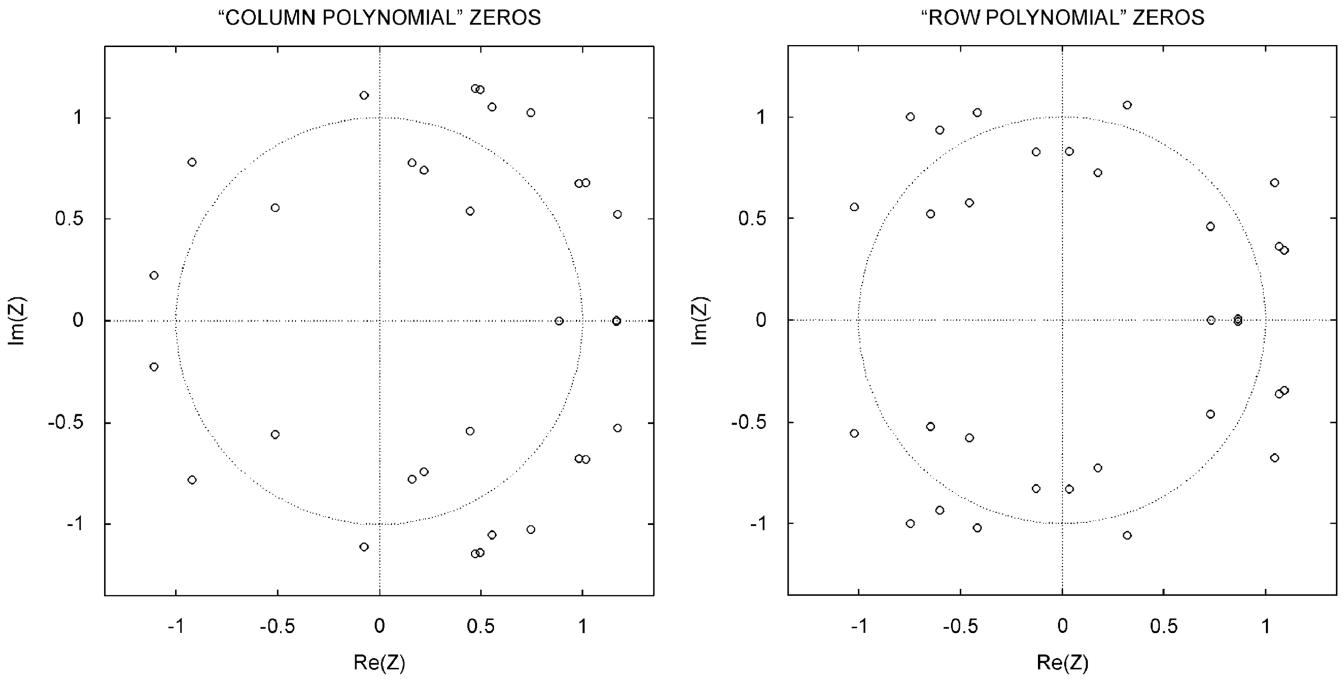

Fig. 1.
(Left) The zeros of the "column" *z*-transform of a separable 32 × 32 sequence. (Right) The zeros of the "row" *z*-transform of the same sequence.

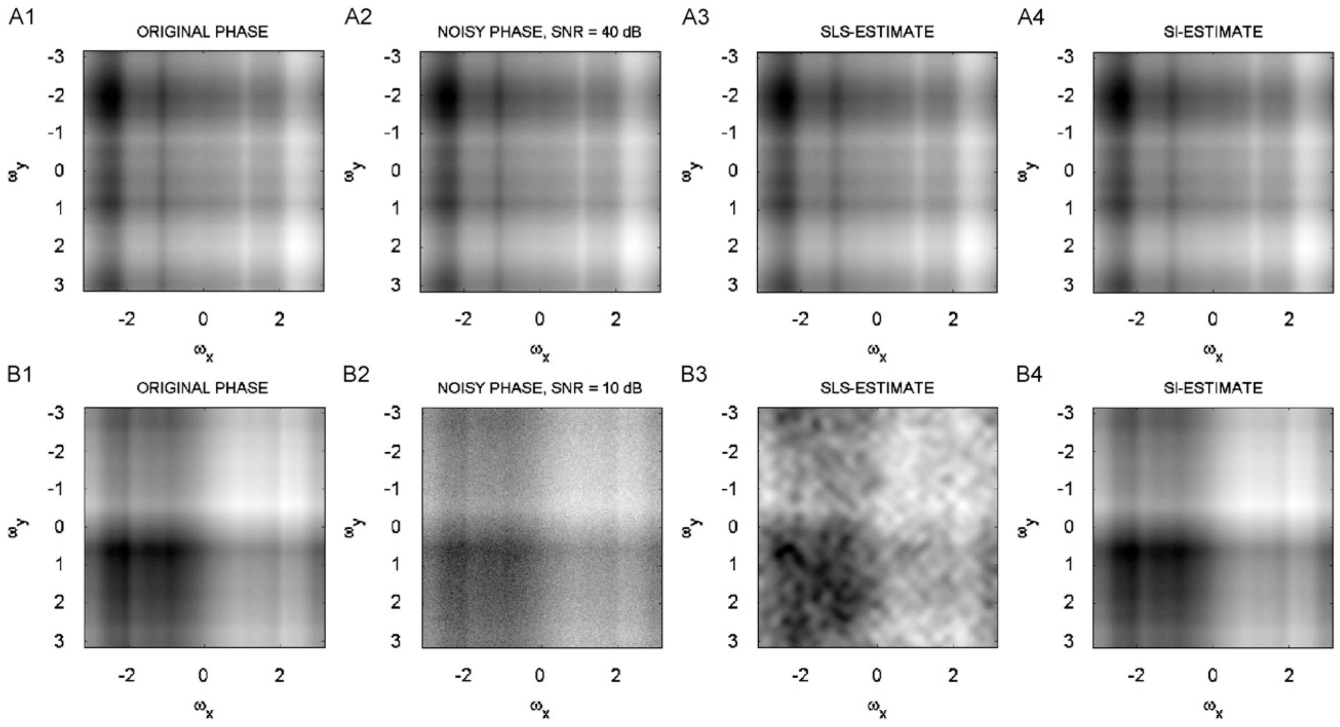

Fig. 2.

(Subplots A1–A4) The original Fourier phase of a simulated sequence, the phase contaminated by 40 dB noise, the SLS and the SI estimate of the phase, respectively. (Subplots B1–B4) The original Fourier phase of a simulated sequence, the phase contaminated by 10 dB noise, the SLS and the SI estimate of the phase, respectively.

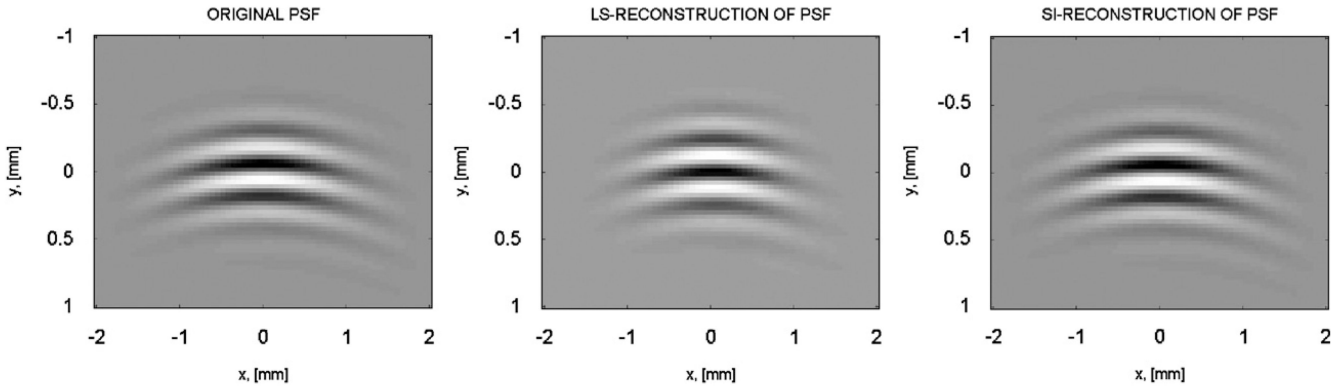

Fig. 3.
(Left) Original PSF. (Center) PSF estimate computed using the SLS method for phase estimation. (Right) PSF estimate computed using the SI method for phase estimation.

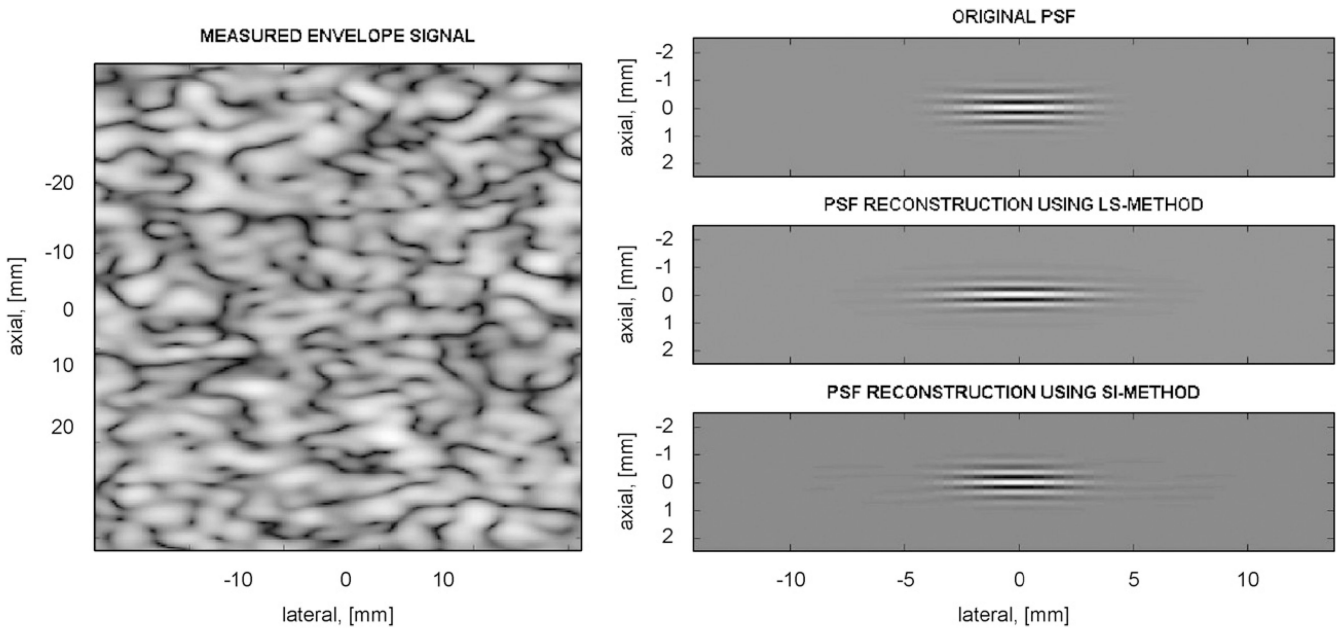

Fig. 4.

(Leftmost subplot) A segment of the envelope of ultrasound data. (Right column of subplots) The measured PSF and its estimates computed using the SLS and SI methods for phase reconstruction.

Table 1

NMSE (±1 standard deviation) of phase estimates obtained at different noise levels for $\phi = B_3$, $J = -5$, and $N = 256$

	SNR = 60 dB	SNR = 40 dB	SNR = 20 dB	SNR = 10 dB
LS	0.0001 ± 0.0000	0.0015 ± 0.0001	0.0222 ± 0.0045	0.3292 ± 0.1778
SLS	0.0111 ± 0.0045	0.0120 ± 0.0054	0.0211 ± 0.0098	0.2682 ± 0.0757
SI	0.0110 ± 0.0044	0.0120 ± 0.0052	0.0130 ± 0.0062	0.0164 ± 0.0076

Table 2

NMSE (±1 standard deviation) of phases estimates obtained for different values of J and for $\phi = B_3$, $N = 256$, and SNR = 15 dB

	$J = -7$	$J = -6$	$J = -5$	$J = -4$	$J = -3$
SLS	0.0605 ± 0.0213	0.0510 ± 0.0175	0.0386 ± 0.0109	0.0856 ± 0.0240	0.1925 ± 0.0349
SI	0.0301 ± 0.0096	0.0174 ± 0.0043	0.0143 ± 0.0039	0.0612 ± 0.0226	0.1585 ± 0.0503

Table 3

NMSE (±1 standard deviation) of phases estimates obtained for different values of N and for $\varphi = B_3$, $J = -5$, and SNR = 15 dB

	$N = 64$	$N = 128$	$N = 256$	$N = 512$
SLS	0.1302 ± 0.0460	0.0978 ± 0.0299	0.0387 ± 0.0107	0.0127 ± 0.0035
SI	0.0237 ± 0.0059	0.0182 ± 0.0048	0.0141 ± 0.0038	0.0122 ± 0.0034

Table 4

NMSE (±1 standard deviation) of phases estimates obtained for different generators ϕ and for $N = 256$, $J = -5$, and SNR = 15 dB

	$\phi = B_2$	$\phi = B_3$	$\phi = B_4$	$\phi = B_5$
SI	0.0144 ± 0.0041	0.0142 ± 0.0039	0.0139 ± 0.0038	0.0134 ± 0.0033

Table 5

NMSE (±1 standard deviation) of PSF estimation for different values of N and for $\phi = B_3$, $J = -5$, and SNR = 15 dB

	$N = 64$	$N = 128$	$N = 256$	$N = 512$
SLS	0.2145 ± 0.0413	0.0912 ± 0.0290	0.0210 ± 0.0079	0.0131 ± 0.0023
SI	0.0476 ± 0.0102	0.0301 ± 0.0130	0.0132 ± 0.0031	0.0130 ± 0.0025